Finite element formulation of variable thickness plates

Babak Ravaji[a]

MEEN 673 – Nonlinear Finite Element Methods

Instructor: Dr. J. N. Reddy[a]

[a] J. Mike Walker ’66 Department of Mechanical Engineering, Texas A&M University, College Station, TX

Introduction

The intense competition between companies especially in automotive industries, pushes the engineers and designers to safer and cheaper products every day. Multi-variable and multi-strength blanks known as Tailor Welded Blanks (TWB’s) are one of the breakthrough improvements in designing and manufacturing of the automotive bodies in the past decade. Mass producing TWB is possible thanks to the advent of fast and reliable laser welding for steel alloys and friction and stir welding for aluminum alloys. Tailor welded blanks are made from individual sheets of steel of different thickness, strength and coating which are joined together by laser welding. This process allows for right properties in the right place [1,2].

Variable thickness sheets are primarily used in automotive industries for side frames, doors, pillars and rails where different strength and performance are anticipated from different sections of these parts. For example the strength expected from the front part of the door inner close to the door hinge is different from that of the rest of the part [3].

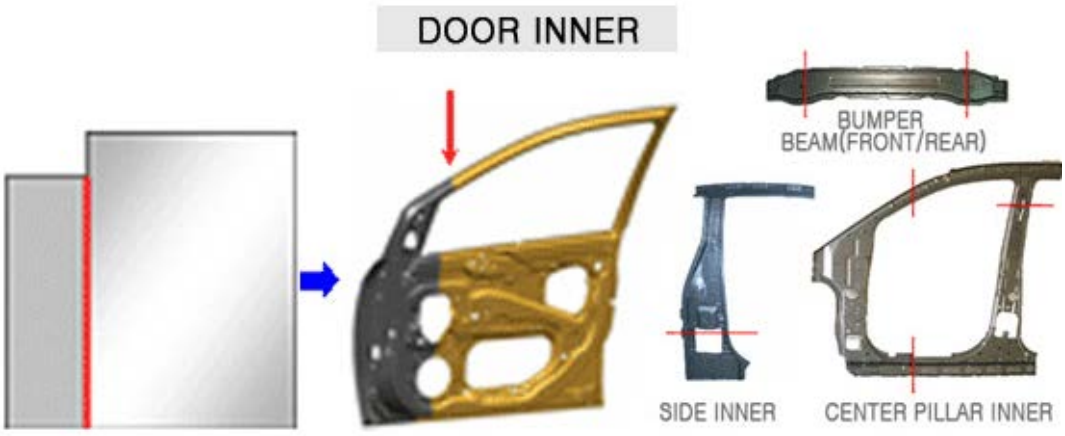

Figure 1. Major usage of TWB in automotive bodies

This technology is not only limited to the mentioned parts. Exploiting TWB technology in the vast majority of the automobile body parts can significantly reduce the number of joining operations and consequently reduce the overall cost of the production [4].

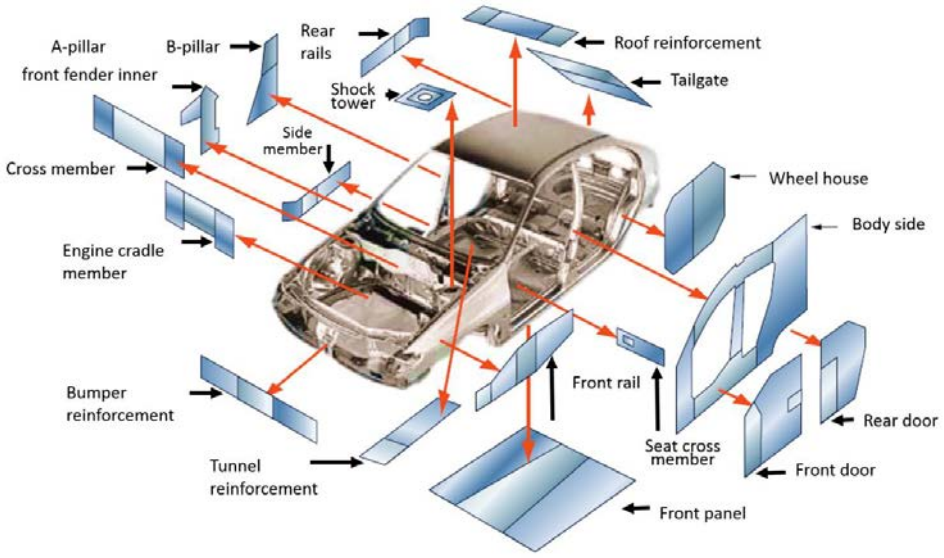

Figure 2. Multi-properties and multi-thickness blanks can be used for many interior body parts.

One other tremendous advantage of TWB is the reduction in the overall weight of the car body. By using appropriate blank thickness in only appropriate regions, it is possible to reduce the weight of some major body parts up to 12% [5].

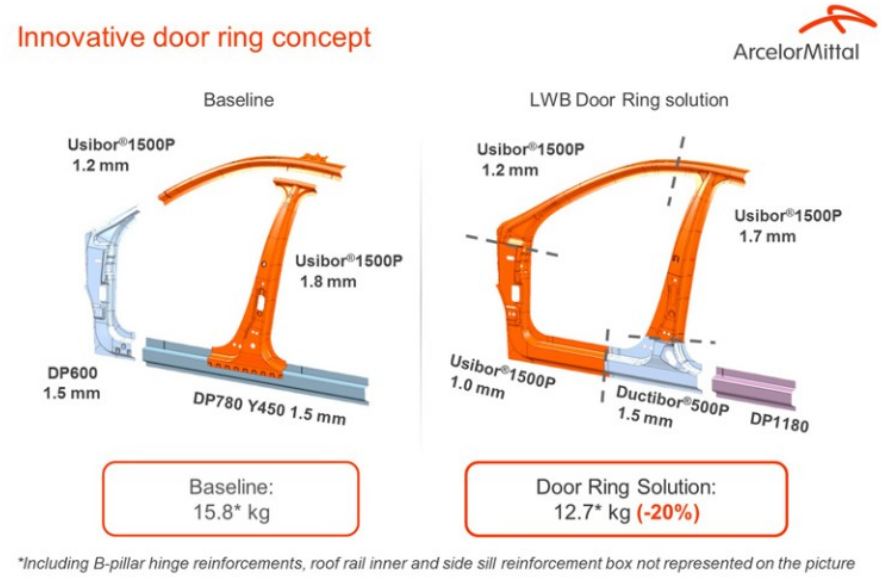

Figure 3. Up to 12% reduction in the assembled parts is achievable.

In this report the governing equations of the first-order shear deformation theory for plates and its application via finite element method in addition to the capability of modeling variable thickness plate is studied.

The first order shear deformation theory

The theory and formulations regarding the first-order shear deformation theory (FSDT) are adopted directly from 'An introduction to nonlinear finite element method' by J. N. Reddy [6]. For more details of FSDT the reader is referred to Reddy [6].

Displacement field

Deformations in 3 directions in FSDT are defined as follows.

$$u_1(x, y, z) = u(x, y) + z\phi_x(x, y)$$
$$u_2(x, y, z) = v(x, y) + z\phi_y(x, y)$$
$$u_3(x, y, z) = w(x, y)$$

where u_1, u_2 and u_3 are displacements along x, y and z directions respectively. Other variables, u, v, and w are depicted in the following figure.

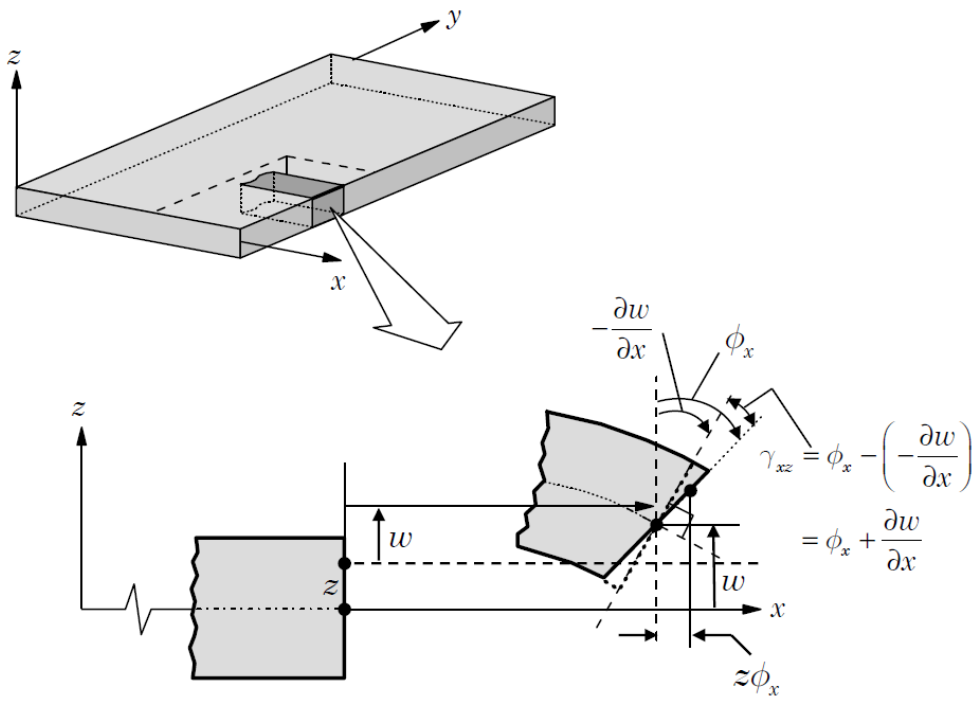

Figure 4. Undeformed and deformed geometries of an edge of a plate under the assumption of FSDT [6].

Weak forms

Weak forms of the equations can be expressed using the virtual work theorem. That said, the internal, external and the total virtual works would be:

$$\delta W_I^e = \int_{\Omega^e} \left\{ \int_{-\frac{h}{2}}^{\frac{h}{2}} \left[\sigma_{xx} \left(\delta\varepsilon_{xx}^0 + z\delta\varepsilon_{xx}^1 \right) + \sigma_{yy} \left(\delta\varepsilon_{yy}^0 + z\delta\varepsilon_{yy}^1 \right) \right.\right.$$
$$\left.\left. + \sigma_{xy} \left(\delta\gamma_{xy}^0 + z\delta\gamma_{xy}^1 \right) + K_s \sigma_{xz} \delta\gamma_{xz}^0 + K_s \sigma_{yz} \delta\gamma_{yz}^0 \right] dz \right\} dx\, dy$$

$$\delta W_E^e = -\left\{ \oint_{\Gamma^e} \int_{-\frac{h}{2}}^{\frac{h}{2}} \left[\sigma_{nn} \left(\delta u_n + z\delta\phi_n \right) + \sigma_{ns} \left(\delta u_s + z\delta\phi_s \right) + \sigma_{nz} \delta w \right] dz\, ds \right.$$
$$\left. + \int_{\Omega^e} \left(q - kw \right) \delta w \; dx\, dy \right\}$$

$$0 = \int_{\Omega^e} \left[N_{xx}\delta\varepsilon_{xx}^0 + M_{xx}\delta\varepsilon_{xx}^1 + N_{yy}\delta\varepsilon_{yy}^0 + M_{yy}\delta\varepsilon_{yy}^1 + N_{xy}\delta\gamma_{xy}^0 \right.$$
$$\left. + M_{xy}\delta\gamma_{xy}^1 + Q_x\delta\gamma_{xz}^0 + Q_y\delta\gamma_{yz}^0 + kw\delta w - q\delta w \right] dx\, dy$$
$$- \oint_{\Gamma^e} \left(N_{nn}\delta u_n + N_{ns}\delta u_s + M_{nn}\delta\phi_n + M_{ns}\delta\phi_s + Q_n\delta w \right) ds$$

where

$$\begin{Bmatrix} N_{xx} \\ N_{yy} \\ N_{xy} \end{Bmatrix} = \begin{bmatrix} A_{11} & A_{12} & 0 \\ A_{12} & A_{22} & 0 \\ 0 & 0 & A_{66} \end{bmatrix} \begin{Bmatrix} \varepsilon_{xx}^0 \\ \varepsilon_{yy}^0 \\ \gamma_{xy}^0 \end{Bmatrix} - \begin{Bmatrix} N_{xx}^T \\ N_{yy}^T \\ 0 \end{Bmatrix}$$

$$\begin{Bmatrix} M_{xx} \\ M_{yy} \\ M_{xy} \end{Bmatrix} = \begin{bmatrix} D_{11} & D_{12} & 0 \\ D_{12} & D_{22} & 0 \\ 0 & 0 & D_{66} \end{bmatrix} \begin{Bmatrix} \varepsilon_{xx}^1 \\ \varepsilon_{yy}^1 \\ \gamma_{xy}^1 \end{Bmatrix} - \begin{Bmatrix} M_{xx}^T \\ M_{yy}^T \\ 0 \end{Bmatrix}$$

$$\begin{Bmatrix} Q_y \\ Q_x \end{Bmatrix} = \begin{bmatrix} A_{44} & 0 \\ 0 & A_{55} \end{bmatrix} \begin{Bmatrix} \gamma_{yz}^0 \\ \gamma_{xz}^0 \end{Bmatrix}$$

and

$$A_{ij} = Q_{ij}\, h, \quad D_{ij} = Q_{ij} \frac{h^3}{12}; \quad A_{44} = K_s G_{23} h, \quad A_{55} = K_s G_{13} h$$
$$Q_{11} = \frac{E_1}{1 - \nu_{12}\nu_{21}}\,, \quad Q_{22} = Q_{11} \frac{E_2}{E_1}\,, \quad Q_{12} = \nu_{12} Q_{22}, \quad Q_{66} = G_{12}$$

As mentioned, equations and formulations are directly adopted from the reference book.

Finite element models of FSDT

The dependent variables and their derivatives are approximated via Lagrangian interpolation functions, that is:

$$u(x,y)=\sum_{j=1}^{m}u_j\psi_j^{(1)}(x,y),\quad v(x,y)=\sum_{j=1}^{m}v_j\psi_j^{(1)}(x,y)$$

$$w(x,y)=\sum_{j=1}^{n}w_j\psi_j^{(2)}(x,y)$$

$$\phi_x(x,y)=\sum_{j=1}^{p}S_j^1\psi_j^{(3)}(x,y),\quad \phi_y(x,y)=\sum_{j=1}^{p}S_j^2\psi_j^{(3)}(x,y)$$

Substituting the interpolation functions into the weak forms of the governing equations the set of nonlinear equations can be expressed as:

$$\begin{bmatrix}\mathbf{K}^{11}&\mathbf{K}^{12}&\mathbf{K}^{13}&\mathbf{K}^{14}&\mathbf{K}^{15}\\ \mathbf{K}^{21}&\mathbf{K}^{22}&\mathbf{K}^{23}&\mathbf{K}^{24}&\mathbf{K}^{25}\\ \mathbf{K}^{31}&\mathbf{K}^{32}&\mathbf{K}^{33}&\mathbf{K}^{34}&\mathbf{K}^{35}\\ \mathbf{K}^{41}&\mathbf{K}^{42}&\mathbf{K}^{43}&\mathbf{K}^{44}&\mathbf{K}^{45}\\ \mathbf{K}^{51}&\mathbf{K}^{52}&\mathbf{K}^{53}&\mathbf{K}^{54}&\mathbf{K}^{55}\end{bmatrix}\begin{Bmatrix}\mathbf{u}^e\\ \mathbf{v}^e\\ \mathbf{w}^e\\ \mathbf{S}^1\\ \mathbf{S}^2\end{Bmatrix}=\begin{Bmatrix}\mathbf{F}^1\\ \mathbf{F}^2\\ \mathbf{F}^3\\ \mathbf{F}^4\\ \mathbf{F}^5\end{Bmatrix}+\begin{Bmatrix}\mathbf{F}^{1T}\\ \mathbf{F}^{2T}\\ \mathbf{0}\\ \mathbf{F}^{4T}\\ \mathbf{F}^{5T}\end{Bmatrix}$$

Where the complete formulations for all K^{ij} are available in the reference book. K_{ij}^{11} and T_{ij}^{13} are brought here as example.

$$K_{ij}^{11}=\int_{\Omega^e}\left(A_{11}\frac{\partial\psi_i^{(1)}}{\partial x}\frac{\partial\psi_j^{(1)}}{\partial x}+A_{66}\frac{\partial\psi_i^{(1)}}{\partial y}\frac{\partial\psi_j^{(1)}}{\partial y}\right)dx\,dy$$

$$T_{ij}^{13} = \sum_{\gamma=1}^{5}\sum_{k=1}^{n(\gamma)} \frac{\partial K_{ik}^{1\gamma}}{\partial w_j}\Delta_k^{\gamma} + K_{ij}^{13} = \sum_{k=1}^{n} \frac{\partial K_{ik}^{13}}{\partial w_j} w_k + K_{ij}^{13}$$

$$= \frac{1}{2}\int_{\Omega^e} \left[\frac{\partial \psi_i^{(1)}}{\partial x}\left(A_{11}\frac{\partial w}{\partial x}\frac{\partial \psi_j^{(2)}}{\partial x} + A_{12}\frac{\partial w}{\partial y}\frac{\partial \psi_j^{(2)}}{\partial y}\right) + A_{66}\frac{\partial \psi_i^{(1)}}{\partial y}\left(\frac{\partial w}{\partial x}\frac{\partial \psi_j^{(2)}}{\partial y} + \frac{\partial w}{\partial y}\frac{\partial \psi_j^{(2)}}{\partial x}\right)\right] dx\, dy + K_{ij}^{13}$$

$$= K_{ij}^{13} + K_{ij}^{13} = 2K_{ij}^{13} = T_{ji}^{31}, \qquad (\mathbf{T}^{13})^{\mathrm{T}} = \mathbf{T}^{31} = \mathbf{K}^{31}$$

Required modifications to FSDT

The FSDT finite element model is obtained without any specific assumptions for the plate thickness or the mechanical properties of the plate. Therefore, the final formulations for stiffness and tangent matrices are still valid for variable plate properties, e.g. variable thickness in this study. The most important modifications to the formulations is applying proper thickness at each element according to its coordinates. That modification is mainly applied through updating A_{ij} and D_{ij} in all equations including all K_{ij} and T_{ij}'s, that is:

$$h = h(x,y), \quad A_{ij} = A_{ij}(x,y), \quad D_{ij} = D_{ij}(x,y)$$

In the following sections, the implementation and simulation results of such problems are discussed.

Computer implementation and FEM results

The finite element model discussed in the report in the next step is implemented in a computer program coded in FORTRAN based on the model that was prepared for the MEEN 673 requirements of assignment 5. The main changes in the code are associated to updating the plate thickness based on the element location in the model.

Next, the model is verified numerically by modeling a fully clamped plate. Because of the symmetric nature of the model, only a quarter of the plate is modeled in this study. The dimensions of the quarter plate model is 5x5 in.

Material properties

Isotropic model is considered in the study with the following values for Young's modulus and Poisson ratio.

$E = 7.8e + 6$ psi

$\nu = 0.3$

Boundary conditions

For the clamped plate the following boundary conditions are applied to the model. The top and right side of the square plate are fixed in all 3 directions and both x and y rotations, that is:

$$u = v = w = \phi_x = \phi_y = 0$$

The symmetry of the model with respect to x and y planes are modeled by fixing lateral displacements and rotation for the left side of the model, and fixing those vertical rotations and displacements for the bottom side of the plate, that is:

The plate right side: $u = \phi_x = 0$

The plate bottom side: $v = \phi_y = 0$

Results

The results of the FEM model for the aforementioned material properties and boundary conditions are shown in the following figures for two different mesh configurations. In the first set of the results a mesh of 4x4 Q9 elements are used and in the second set of results the same model is meshed with 8x8 L4 elements.

4x4 Q9 elements

Vertical displacement of the nodes are shown in the following figures. From top left to bottom right the following thickness configurations are applied to the model:

1. Thickness is constant all through the model (h=1).
2. There is a jump in the plate thickness from x=2.5. In the left side h=1, and on the right side h=2 Is applied.
3. The plate thickness is gradually increasing along the x axis such that it is 1 at x=0 and 6 at x=5.
4. The model thickness is radially increasing with the same slope as in the previous case.

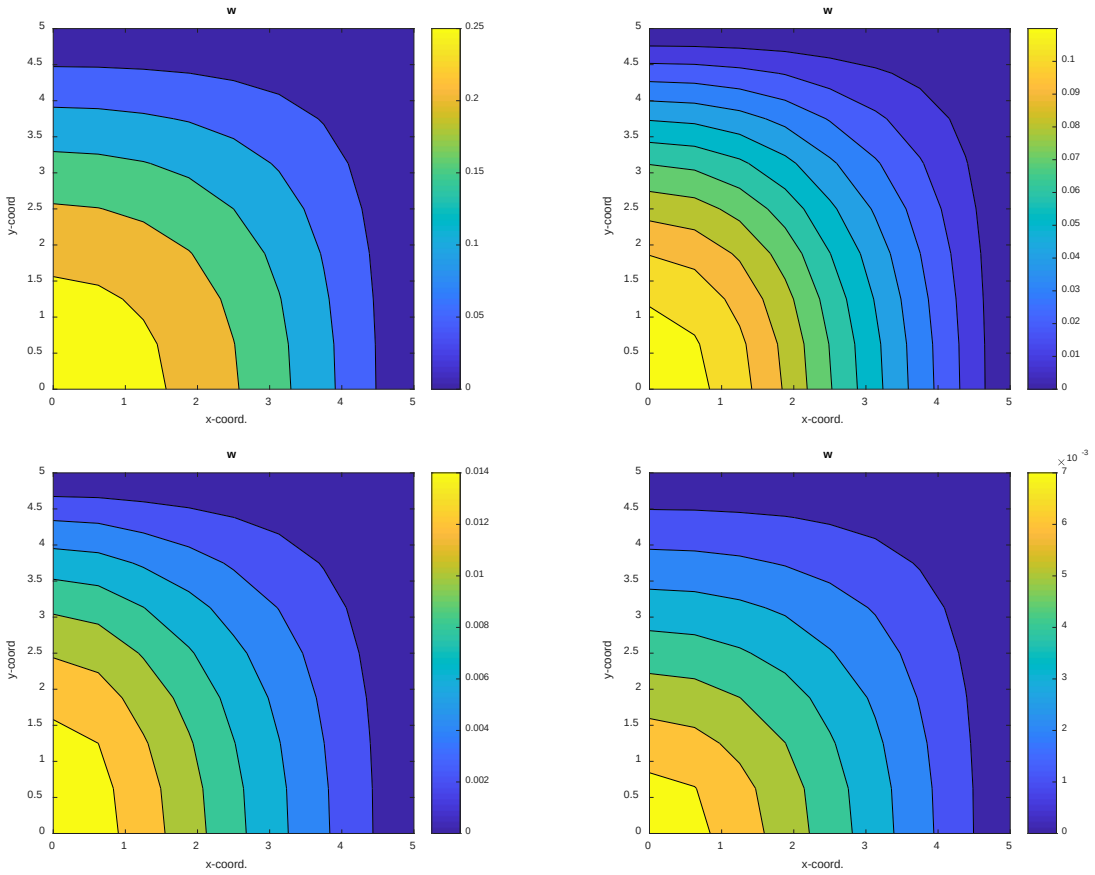

Figure 5. Vertical displacement of the clamped plate, 4x4 Q9 elements.

As it is expected the vertical displacement is decreasing as the model thickness is increasing. The effect of the jump discontinuity in the thickness in the second model is not seen very well although the magnitude of decreasing of the displacement is apparent. The difference between the first two cases is seen well when in the following the stresses are compared.

Cases 1 and 4 are symmetric with respect to x and axes and therefore the displacement contours are also symmetric with respect to the origin point. However in cases 2 and 3 the model thickness is not symmetric with respect t oy axis and that is why the contour plots are also unsymmetrical.

In the following set of figures σ_{xx} in the four different model are depicted. Similar to the vertical displacement results the magnitude of the stress is decreasing as the plate thickness is increasing.

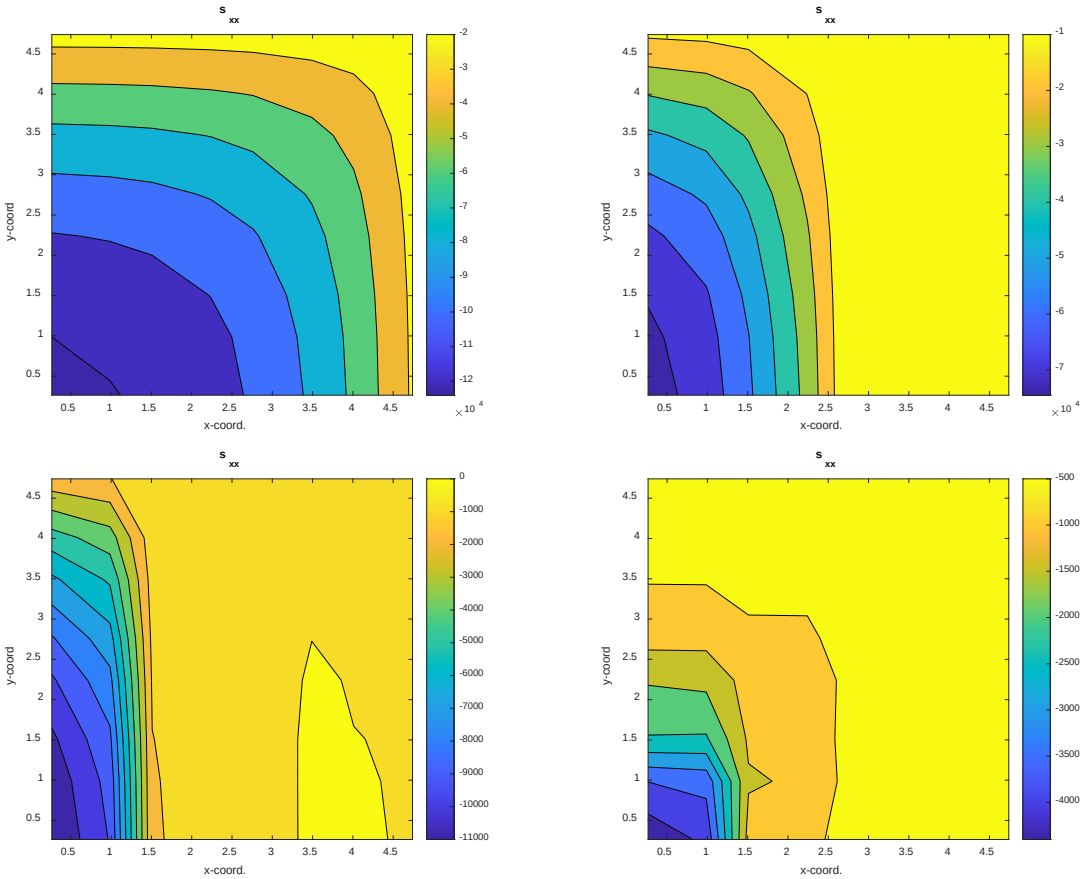

Figure 6. Horizontal stress, σ_{xx} , of the clamped plate, 4x4 Q9 elements

Comparing σ_{xx}, the difference between cases 1 and 2, and the effect of the discontinuity in the model thickness is more apparent.

One important point in the stress results shown in the previous and the following figure for σ_{yy} is that the model mesh is not fine enough to capture a smooth stress contours in case 4 where thickness is linearly increasing radially from the plate origin.

The results for σ_{yy} are more or less the same as those shown for σ_{xx} before with the same trends and the dame mesh deficiencies.

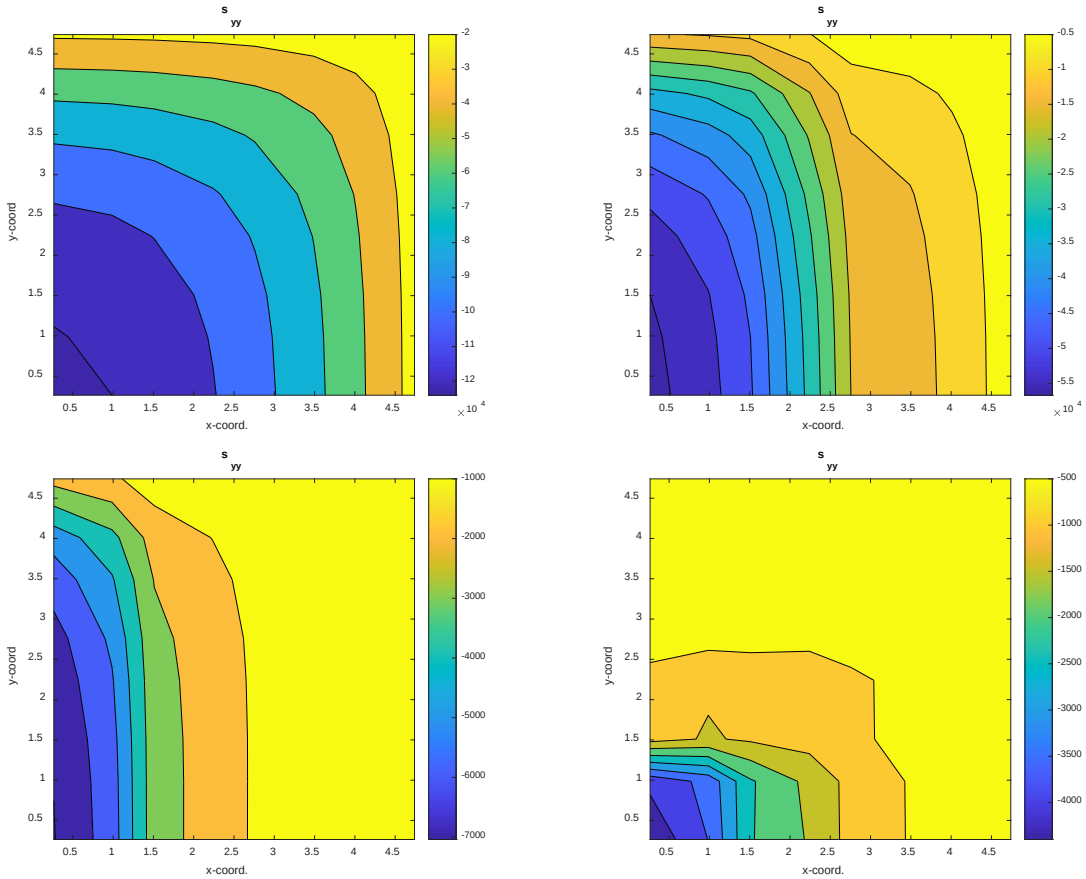

Figure 7. Vertical stress, σ_{yy} , of the clamped plate, 4x4 Q9 elements

In order to achieve better and smoother stress results and being able to compare results, in the next section the same simulations are repeated based upon 8x8 L4 elements mesh.

8x8 L4 elements

The same results for the mesh of 8x8 linear elements are shown in the following figures. It is expected to achieve smoother displacement and stress results because of better distribution of the plate thickness. That is mainly because my finite element model for considering variable thickness works in an element-based computations, that is, each elements has only one thickness. Therefore, when the number of elements despite reducing the order of elements from quadratic to linear, smoother thickness variation and hence smoother stress and displacements are anticipated.

In the following set of figures results for vertical displacements are shown. Comparing it with those presented earlier in the previous section, the displacement results for 4x4 Q9 and 8x8 L4 mesh configurations are identical.

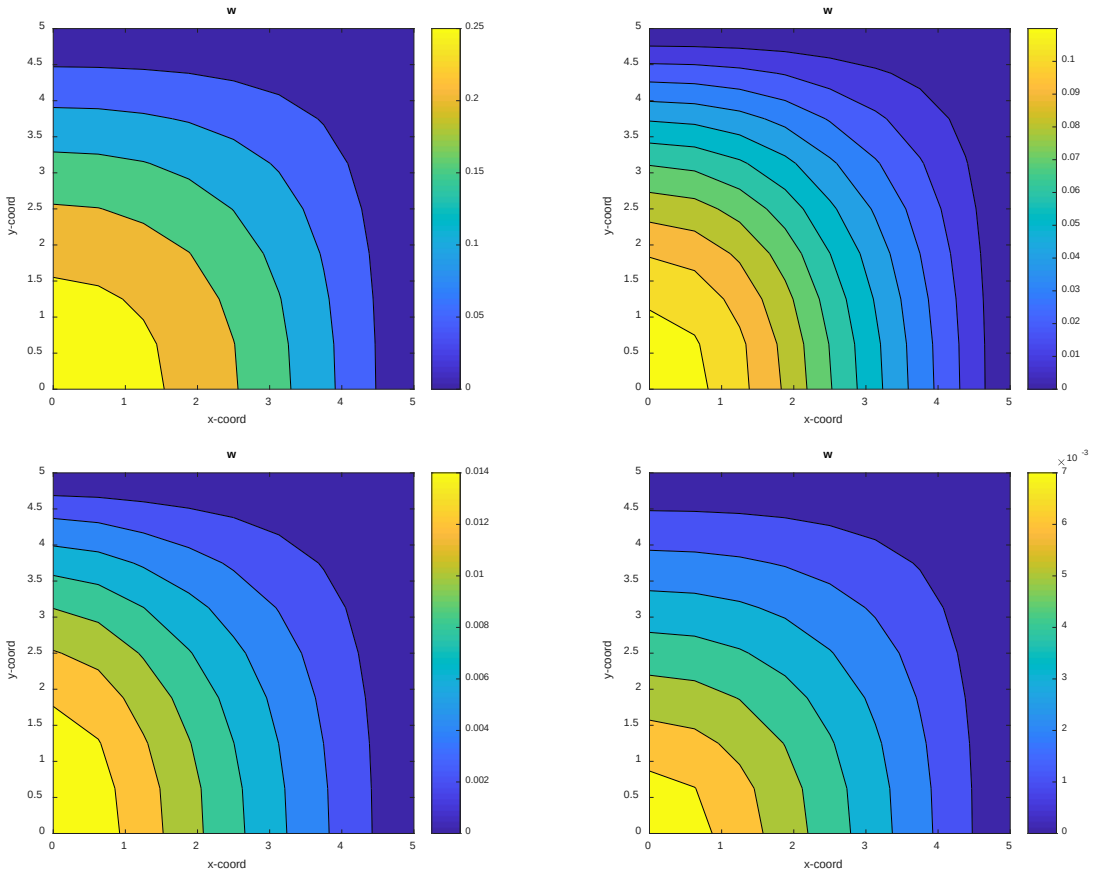

Figure 8. Vertical displacement of the clamped plate, 8x8 L4 elements.

Nonetheless, when it comes to stress comparisons, the results for 8x8 L4 elements are much smoother. In the following set of figures the stress output values, σ_{xx} and σ_{yy}, are shown. The zig-zag un-smooth stress contours for radial thickness change is solves completely by increasing the number of elements.

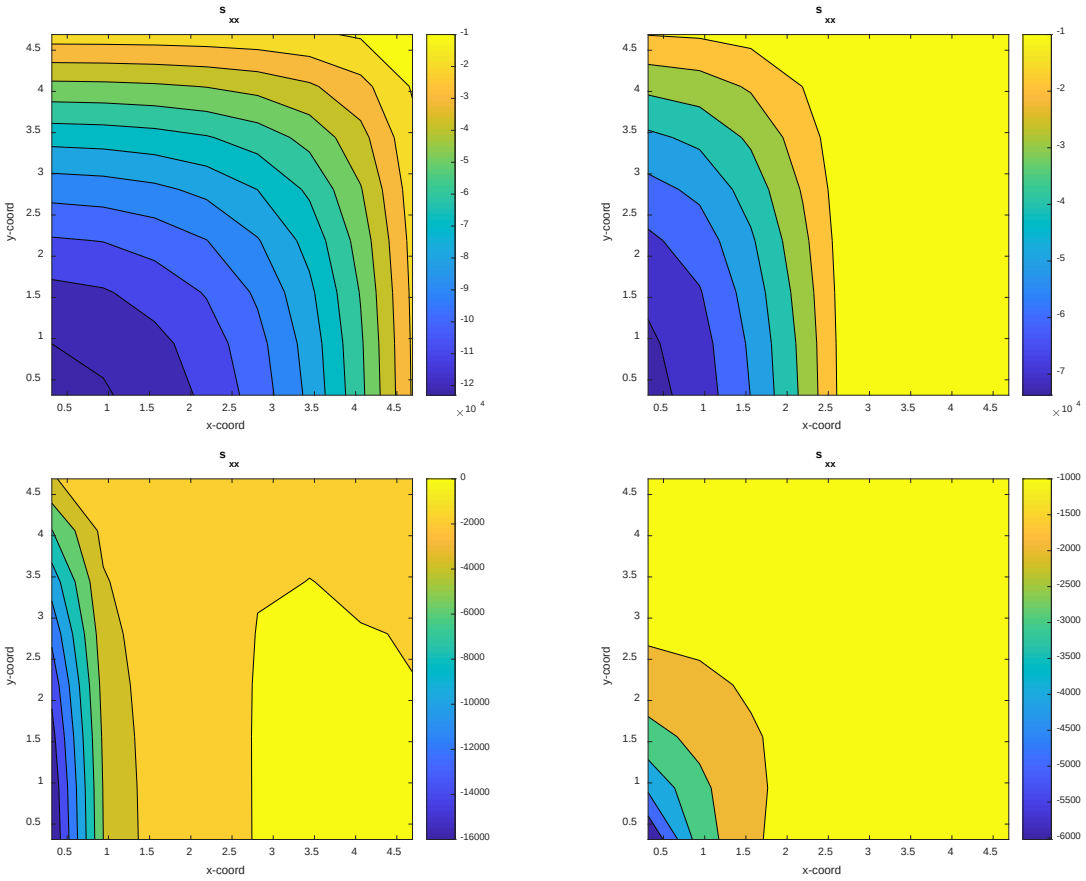

Figure 9. Horizontal stress, σ_{xx} , of the clamped plate, 8x8 L4 elements

In order to achieve more reliable and accurate stress results for the introduced plate configurations more mesh dependency studies is suggested.

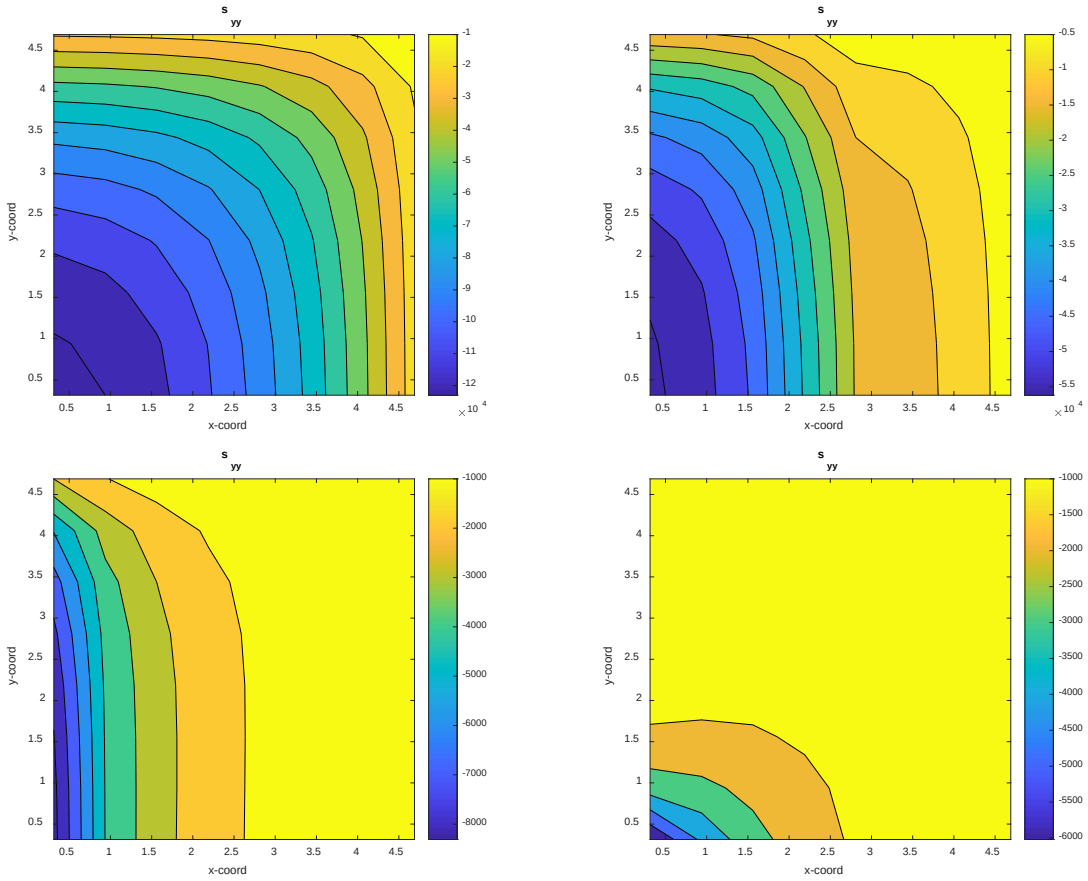

Figure 10. Vertical stress, σ_{yy} , of the clamped plate, 8x8 L4 elements

Conclusions

The variable thickness plate models have a vast applications especially in the automotive industries. The FEM model presented in the current report provides the essential requirements for modeling such plates for any arbitrary thickness variation in the plate. The model is then tested for 3 different scenarios and stress and displacement outputs are then compared with those of constant thickness.

At the end more model verifications for studying mesh dependency of the model are suggested. The next step in completing the capabilities of the model could be implementation of shell theory in the code in addition to the current FSDT model.

References

1. https://www.twbcompany.com/
2. http://www.cc-ceck.com/
3. https://en.wikipedia.org/wiki/Tailored_blank
4. Kashani et. al. Laser overlap welding of zinc coated steel on aluminum alloy, **2015**, Physics Procedia
5. https://corporate.arcelormittal.com/
6. J. N. Reddy, An introduction to nonlinear finite element analysis, **2015**, Oxford university press